

Sliced gradient-enhanced Kriging for high-dimensional function approximation

Kai Cheng¹ and Ralf Zimmermann²

Abstract

Gradient-enhanced Kriging (GE-Kriging) is a well-established surrogate modelling technique for approximating expensive computational models. However, it tends to get impractical for high-dimensional problems due to the large inherent correlation matrix and the associated high-dimensional hyper-parameter tuning problem. To address these issues, we propose a new method in this paper, called sliced GE-Kriging (SGE-Kriging) for reducing both the size of the correlation matrix and the number of hyper-parameters. Firstly, we perform a derivative-based global sensitivity analysis to detect the relative importance of each input variable with respect to model response. Then, we propose to split the training sample set into multiple slices, and invoke Bayes' theorem to approximate the full likelihood function via a sliced likelihood function, in which multiple small correlation matrices are utilized to describe the correlation of the sample set. Additionally, we replace the original high-dimensional hyper-parameter tuning problem with a low-dimensional counterpart by learning the relationship between the hyper-parameters and the global sensitivity indices. Finally, we validate SGE-Kriging by means of numerical experiments with several benchmarks problems. The results show that the SGE-Kriging model features an accuracy and robustness that is comparable to the standard one but comes at much less training costs. The benefits are most evident in high-dimensional problems.

Keywords: Gradient-enhanced Kriging, Surrogate modeling, Maximum likelihood estimation, Global sensitivity analysis, Hyper-parameter tuning

¹Postdoc, Department of Mathematics and Computer Science, University of Southern Denmark (SDU), kai@sdu.dk

²Associated professor, Department of Mathematics and Computer Science, University of Southern Denmark (SDU), zimmermann@imada.sdu.dk

1. Introduction

Surrogate models have been widely applied to alleviate the heavy computational burden in the field of design, control, optimization and uncertainty quantification, where expensive high-fidelity numerical simulation models are employed to study and simulate the underlying physical phenomena of various complex systems [27]. A surrogate model, also known as a meta-model, is an interpolation or regression model based on sampled data that is to mimic the behavior of system responses with respect to selected input parameters, and it can be used to predict the response of the expensive simulation model at any untried point efficiently. In the past decades, various surrogate modelling techniques have been developed, including Kriging [19, 11, 30], support vector regression [33, 32, 8], polynomial chaos expansion [36, 3, 7], neural networks [1, 14] and so on. Among these approaches, Kriging has drawn the most attention in engineering applications due to its attractive statistical properties and its flexibility and extensibility.

Kriging assumes that the system response is a realization of a Gaussian process [19, 28], and it can be fully described by the associated mean and covariance functions. The mean function is used to capture the global trend of a computational model. The covariance function, arguably the most important ingredient of Kriging, describes the spatial dependence between different sample points. Under the Gaussian process assumption, Kriging provides point-wise probabilistic prediction and error bars to account for the epistemic uncertainty, which makes it convenient to combine the method with adaptive sampling strategies for various scenarios [16].

As with other surrogate techniques, Kriging suffers from the so-called “curse of dimensionality”, namely, the size of the sample set required to train an accurate Kriging model increases exponentially with the input dimension. To alleviate this problem, gradient-enhanced Kriging (GE-Kriging) has been developed. The idea is to incorporate gradient information, obtained, say, with adjoint methods [2] or automatic differentiation [26], to enhance the accuracy of the Kriging model [10, 25].

There are two basic versions of GE-Kriging in the literature, namely, indirect GE-Kriging and direct GE-Kriging. In indirect GE-Kriging [24, 23], the gradient information is used to construct additional sample values and corresponding function values near the existing sampling sites by a first-

order Taylor’s expansion. However, this method will introduce additional numerical errors and is observed to result in ill-conditioned correlation matrices, which may undermine the performance of GE-Kriging. In contrast, by assuming that the system responses and its partial derivative functions are realizations of Gaussian processes, the direct GE-Kriging [12, 4, 13, 6] is constructed by absorbing the correlations between function values and the cross-correlations between function values and partial derivatives directly. Consequently, direct GE-Kriging is superior to the indirect approach in theory, and the corresponding correlation matrix is relatively well-conditioned [13, 38]. Therefore, direct GE-Kriging is investigated in current work.

Although GE-Kriging seems appealing to break the “curse of dimensionality”, practical applications suggest that it suffers from two drawbacks in the context of high-dimensional problems. On the one hand, the correlation matrix of GE-Kriging is largely expanded, which makes it costly to deal with, especially when it comes to solving linear equation systems that involve the correlation matrix as the operator. On the other hand, the likelihood function of GE-Kriging is generally highly non-linear and contains multiple extrema, which makes it very challenging to tune the hyper-parameters of GE-Kriging by maximum likelihood estimation. As a consequence, training a GE-Kriging model can be extremely time-consuming for high-dimensional problems. This motivates researchers towards improving the efficiency of constructing GE-Kriging. Bouhle et al. [4] proposed to reduce the size of the correlation matrix of GE-Kriging as well as the number of hyper-parameters by utilizing a partial least-squares regression technique. Similarly, Chen et al. [5] suggested to reduce the correlation matrix in size by incorporating a part of the partial derivatives that is identified by a feature selection technique. In [13], Han et al. proposed to train a series of submodels using only a part of the training sample set, and then to sum them up with appropriate weight coefficients to provide predictions.

In this paper, we develop a new method, called sliced GE-Kriging (SGE-Kriging) to improve the training efficiency of standard GE-Kriging for high-dimensional problems. We firstly utilize a derivative-based global sensitivity analysis method [15, 21] to explore the relative importance of every input variable with respect to the system response. Then, using Bayes’ theorem, a simplified likelihood function is derived that neglects the correlation between samples that are far away from each other. Further, the number of hyper-parameters in the SGE-Kriging model is reduced by learning a preset functional relationship between the model hyper-parameter and the global

sensitivity indices. Finally, several benchmarks are investigated to demonstrate the performance of SGE-Kriging.

The remainder of this paper is organized as follows. In Section 2, we review the basic theory of GE-Kriging including the underlying assumptions, the key equations, the hyper-parameter tuning approach and the associated correlation functions. Then, the novel SGE-Kriging is introduced in Section 3. The derivative-based global sensitivity analysis method and the proposed sliced likelihood function are presented in Subsections 3.1 and 3.2, respectively, followed by the simplified hyper-parameter tuning method in Section 3.3. We then compare the performance of the SGE-Kriging approach to the classical GE-Kriging in Section 4 by means of several numerical benchmark examples of increasing sophistication. Finally, we summarize our observations and conclusions in Section 5.

2. A recap of the gradient-enhanced Kriging framework

In this section, we review the basic principles of GE-Kriging, followed by a recap of the hyper-parameter tuning technique and the correlation function models used in GE-Kriging.

2.1. The gradient-enhanced Kriging model

Consider a computational multiple input-single output process $y = g(\mathbf{x})$, where $\mathbf{x} = (x_1, \dots, x_n)^T$ is the input parameter vector, and y is the scalar model response. GE-Kriging is concerned with approximating $g(\mathbf{x})$ by a model based on a set of observed samples (\mathbf{X}, \mathbf{y}) , where \mathbf{X} is a matrix of N sample sites $\mathbf{x}^{(i)} \in \mathbb{R}^n$, and \mathbf{y} is a response vector that contains the observed function values as well as the gradients at the sample sites, i. e.,

$$\mathbf{X} = [\mathbf{x}^{(1)}, \dots, \mathbf{x}^{(N)}]^T \in \mathbb{R}^{N \times n},$$

$$\mathbf{y} = [\mathbf{y}_0^T, \mathbf{y}_1^T, \dots, \mathbf{y}_n^T]^T \in \mathbb{R}^{(n+1)N},$$

in which

$$\mathbf{y}_0 = [g(\mathbf{x}^{(1)}), g(\mathbf{x}^{(2)}), \dots, g(\mathbf{x}^{(N)})]^T \in \mathbb{R}^N,$$

$$\mathbf{y}_k = \left[\frac{\partial g(\mathbf{x}^{(1)})}{\partial x_k}, \frac{\partial g(\mathbf{x}^{(2)})}{\partial x_k}, \dots, \frac{\partial g(\mathbf{x}^{(N)})}{\partial x_k} \right]^T \in \mathbb{R}^N, \quad k = 1, \dots, n.$$

In GE-Kriging, the computational model $y = g(\mathbf{x})$ is regarded as a realization of a spatial Gaussian process $Y(\mathbf{x})$ that is given by a regression model

and an additive Gaussian error term. In the case of constant regression, this means that

$$Y(\mathbf{x}) = \beta_0 + Z(\mathbf{x}), \quad (1)$$

where β_0 is the regression constant that represents the mean value of $Y(\mathbf{x})$, and $Z(\mathbf{x})$ is a stationary Gaussian process with zero mean and covariance function

$$\text{Cov}(Z(\mathbf{x}), Z(\hat{\mathbf{x}})) = \sigma^2 R(\mathbf{x}, \hat{\mathbf{x}}; \boldsymbol{\theta}).$$

In the latter, σ^2 is the stationary variance of $Z(\mathbf{x})$, and $R(\mathbf{x}, \hat{\mathbf{x}}; \boldsymbol{\theta})$ represents the spatial correlation between two points \mathbf{x} and $\hat{\mathbf{x}}$ with the correlation lengths being controlled by the hyper-parameter vector $\boldsymbol{\theta}$.

The partial derivative functions $\frac{\partial Z(\mathbf{x})}{\partial x_k}$ ($k = 1, \dots, n$) of $Z(\mathbf{x})$ are again Gaussian processes, and the cross-covariance functions between the different Gaussian processes are given by the partial derivatives of the correlation function, see, e. g., [17, §4.5] or [35, §4.1]:

$$\begin{aligned} \text{Cov}\left(\frac{\partial Z(\mathbf{x})}{\partial x_k}, Z(\hat{\mathbf{x}})\right) &= \sigma^2 \frac{\partial R(\mathbf{x}, \hat{\mathbf{x}}; \boldsymbol{\theta})}{\partial x_k}, \quad k = 1, \dots, n, \\ \text{Cov}\left(Z(\mathbf{x}), \frac{\partial Z(\hat{\mathbf{x}})}{\partial \hat{x}_l}\right) &= \sigma^2 \frac{\partial R(\mathbf{x}, \hat{\mathbf{x}}; \boldsymbol{\theta})}{\partial \hat{x}_l}, \quad l = 1, \dots, n, \\ \text{Cov}\left(\frac{\partial Z(\mathbf{x})}{\partial x_k}, \frac{\partial Z(\hat{\mathbf{x}})}{\partial \hat{x}_l}\right) &= \sigma^2 \frac{\partial^2 R(\mathbf{x}, \hat{\mathbf{x}}; \boldsymbol{\theta})}{\partial x_k \partial \hat{x}_l}, \quad k, l = 1, \dots, n. \end{aligned}$$

Under the Gaussian process assumption, the joint distribution of $Y(\mathbf{x})$ and $\mathbf{Y} = [Y(\mathbf{x}^{(1)}), \dots, Y(\mathbf{x}^{(N)}), \frac{\partial Y(\mathbf{x}^{(1)})}{\partial x_1}, \dots, \frac{\partial Y(\mathbf{x}^{(N)})}{\partial x_1}, \dots, \frac{\partial Y(\mathbf{x}^{(1)})}{\partial x_n}, \dots, \frac{\partial Y(\mathbf{x}^{(N)})}{\partial x_n}]^T$ at all the sampling sites is multivariate Gaussian [22], namely

$$\begin{bmatrix} Y(\mathbf{x}) \\ \mathbf{Y} \end{bmatrix} \sim \mathcal{N}\left(\begin{bmatrix} \beta_0 \\ \beta_0 \mathbf{F} \end{bmatrix}, \sigma^2 \begin{bmatrix} 1 & r^T(\mathbf{x}) \\ r(\mathbf{x}) & \mathbf{R} \end{bmatrix}\right),$$

where

$$\mathbf{F} = \underbrace{[1, \dots, 1]}_N, \underbrace{[0, \dots, 0]}_{nN}^T \in \mathbb{R}^{(n+1)N}$$

for constant regression. In the case of a general regression model, \mathbf{F} is to be replaced with a regression design matrix, see [38, §2.3].

The matrix

$$\mathbf{R} = \begin{bmatrix} \mathbf{R}_{0,0} & \partial\mathbf{R}_{0,1} & \cdots & \partial\mathbf{R}_{0,n} \\ \partial\mathbf{R}_{1,0} & \partial^2\mathbf{R}_{1,1} & \cdots & \partial^2\mathbf{R}_{1,n} \\ \vdots & \vdots & \ddots & \vdots \\ \partial\mathbf{R}_{n,0} & \partial^2\mathbf{R}_{n,1} & \cdots & \partial^2\mathbf{R}_{n,n} \end{bmatrix} \in \mathbb{R}^{(n+1)N \times (n+1)N}$$

represents the correlation matrix of \mathbf{Y} , and its elements are given by

$$\begin{aligned} \mathbf{R}_{0,0} &:= R(\mathbf{x}^{(i)}, \mathbf{x}^{(j)}; \boldsymbol{\theta}), \quad i, j = 1, \dots, N, \\ \partial\mathbf{R}_{0,k} = \partial\mathbf{R}_{k,0}^T &:= \frac{\partial R(\mathbf{x}^{(i)}, \mathbf{x}^{(j)}; \boldsymbol{\theta})}{\partial x_k^{(j)}}, \quad i, j = 1, \dots, N; k = 1, \dots, n, \\ \partial^2\mathbf{R}_{k,l} &:= \frac{\partial^2 R(\mathbf{x}^{(i)}, \mathbf{x}^{(j)}; \boldsymbol{\theta})}{\partial x_k^{(i)} \partial x_l^{(j)}}, \quad i, j = 1, \dots, N; k, l = 1, \dots, n. \end{aligned}$$

Moreover, $r(\mathbf{x}) = [r_0(\mathbf{x})^T, \partial r_1(\mathbf{x})^T, \dots, \partial r_n(\mathbf{x})^T]^T \in \mathbb{R}^{(n+1)N}$ is the correlation vector between $Y(\mathbf{x})$ and \mathbf{Y} , in which

$$\begin{aligned} r_{0,i}(\mathbf{x}) &:= R(\mathbf{x}^{(i)}, \mathbf{x}; \boldsymbol{\theta}), \quad i = 1, \dots, N, \\ \partial r_{k,i}(\mathbf{x}) &:= \frac{\partial R(\mathbf{x}^{(i)}, \mathbf{x}; \boldsymbol{\theta})}{\partial x_k}, \quad i = 1, \dots, N; k = 1, \dots, n. \end{aligned}$$

Given the observation $\mathbf{Y} = \mathbf{y}$, the posterior predictive distribution $\hat{Y}(\mathbf{x})$ of $Y(\mathbf{x})$ is still Gaussian, namely

$$\hat{Y}(\mathbf{x}) \sim \mathcal{N}(\mu(\mathbf{x}), s^2(\mathbf{x})), \quad (2)$$

where

$$\mu(\mathbf{x}) = \beta_0 + r^T(\mathbf{x})\mathbf{R}^{-1}(\mathbf{y} - \beta_0\mathbf{F}), \quad (3)$$

and

$$s^2(\mathbf{x}) = \sigma^2 \left(1 - r^T(\mathbf{x})\mathbf{R}^{-1}r(\mathbf{x}) + (1 - \mathbf{F}^T\mathbf{R}^{-1}r(\mathbf{x}))^2 / (\mathbf{F}^T\mathbf{R}^{-1}\mathbf{F}) \right). \quad (4)$$

The mean function $\mu(\mathbf{x})$ serves as the surrogate model, and the variance function $s^2(\mathbf{x})$ measures the prediction uncertainty at the location \mathbf{x} .

2.2. Maximum likelihood estimation

The performance of GE-Kriging depends on a number of parameters, namely, the regression constant β_0 , the process variance σ^2 and the hyper-parameters $\boldsymbol{\theta}$. These parameters are generally tuned by the maximum likelihood estimation method. The likelihood function of GE-Kriging is

$$f(\mathbf{y}) = \frac{1}{\sqrt{(2\pi\sigma^2)^{(n+1)N} [\det\mathbf{R}(\boldsymbol{\theta})]}} \exp \left(-\frac{1}{2\sigma^2} (\mathbf{y} - \beta_0\mathbf{F})^T \mathbf{R}^{-1}(\boldsymbol{\theta}) (\mathbf{y} - \beta_0\mathbf{F}) \right). \quad (5)$$

After taking the logarithm of Eq. (5), the optimal profile lines of β_0 and σ^2 depending on $\boldsymbol{\theta}$ can be derived analytically. This yields

$$\beta_0(\boldsymbol{\theta}) = (\mathbf{F}^T \mathbf{R}^{-1}(\boldsymbol{\theta}) \mathbf{F})^{-1} \mathbf{F}^T \mathbf{R}^{-1}(\boldsymbol{\theta}) \mathbf{y}, \quad (6)$$

$$\sigma^2(\boldsymbol{\theta}) = \frac{1}{(n+1)N} (\mathbf{y} - \beta_0(\boldsymbol{\theta}) \mathbf{F})^T \mathbf{R}^{-1}(\boldsymbol{\theta}) (\mathbf{y} - \beta_0(\boldsymbol{\theta}) \mathbf{F}), \quad (7)$$

see, e.g, [12]. There is no closed-form solutions for the optimal hyper-parameters $\boldsymbol{\theta} = [\theta_1, \dots, \theta_n]^T \in \mathbb{R}^n$, and one has to use numerical optimization algorithms to determine their values. Substituting the optimal values of $\beta_0(\boldsymbol{\theta})$ and $\sigma^2(\boldsymbol{\theta})$ into the likelihood function in Eq. (5), we are left with minimizing the following $\boldsymbol{\theta}$ -dependent likelihood function

$$\ell(\boldsymbol{\theta}) = (n+1)N \ln \sigma^2(\boldsymbol{\theta}) + \ln [\det \mathbf{R}(\boldsymbol{\theta})]. \quad (8)$$

To numerically evaluate this function, one needs to deal with a large, possibly ill-conditioned correlation matrix $\mathbf{R} \in \mathbb{R}^{(n+1)N \times (n+1)N}$. When a Cholesky factorization is used to decompose \mathbf{R} , the corresponding computational costs are $\mathcal{O}((n+1)^3 N^3)$, which tends to be very time-consuming for large number of samples N and a large spatial dimension n . Moreover, the computations are unstable.

2.3. Correlation function

In GE-Kriging, any twice continuously differentiable correlation function can be used. In general, a multivariate correlation function can be obtained via the tensor product of univariate ones, namely

$$R(\mathbf{x}, \hat{\mathbf{x}}; \boldsymbol{\theta}) = \prod_{k=1}^n R(|x_k - \hat{x}_k|; \theta_k), \quad (9)$$

where the inputs $\mathbf{x}, \hat{\mathbf{x}}$ are n -vectors and $R(|x_k - \hat{x}_k|; \theta_k)$ denotes the one-dimensional spatial correlation function.

Although the Gaussian correlation function is popular in Kriging, it is known to lead to exceptionally ill-conditioned correlation matrices [39]. In contrast, the cubic spline and biquadratic spline correlation functions have been demonstrated to be comparably well-conditioned [13, 29]. Based on our own numerical experiments (see the discussion in Section 4.1) and the literature [29], the biquadratic splines generally yield smoother and simpler likelihood functions when compared to the cubic spline correlation function. Therefore, the biquadratic spline correlation function is employed in this paper; the associated formulas are to be found in Appendix A.

3. Sliced gradient-enhanced Kriging

As mentioned previously, although the accuracy of a Kriging model can be improved significantly by incorporating gradient information, GE-Kriging suffers from two drawbacks for high-dimensional problems. First, the dimension of the correlation matrix of GE-Kriging is expanded from $N \times N$ to $N(n+1) \times N(n+1)$, when compared to Kriging. Second, as with Kriging, the likelihood function of GE-Kriging in Eq. (8) generally contains multiple local minima in the high-dimensional space, and thus the hyper-parameter tuning process is numerically challenging. In this section, we will introduce a modified approach, which we refer to as *sliced gradient-enhanced Kriging* (SGE-Kriging), with which we aim to address both the two aforementioned deficiencies of GE-Kriging simultaneously.

3.1. Derivative-based global sensitivity analysis

Global sensitivity analysis aims at detecting a comparably small group of input variables that are deemed “important” from the tremendous candidate set of input variables. This is achieved by quantifying the impact of the input variables onto the model response [9, 34, 31]. Since we work under the assumption that gradient information is available, it is convenient to use the derivative-based global sensitivity analysis method in the work at hand. We employ the derivative-based global sensitivity index from [15, 21], which is defined as

$$S_k = \int_{\mathbb{R}^n} \left(\frac{\partial g(\mathbf{x})}{\partial x_k} \right)^2 \rho(\mathbf{x}) d\mathbf{x}, \quad (10)$$

where $\rho(\mathbf{x})$ is the joint probability density function of \mathbf{x} . Note that S_k measures the variability of $g(\mathbf{x})$ in the k -th coordinate direction. For input variables with large sensitivity index, one can deduce that $g(\mathbf{x})$ varies dramatically along the corresponding coordinate direction. In contrast, $g(\mathbf{x})$ is close to constant in the directions with small sensitivity index. Therefore, global sensitivity analysis allows us to detect a low-dimensional subspace within which the model response exhibits strong variability. The subspace dimension $n' < n$ is called the effective dimension of $g(\mathbf{x})$ [20]. Since GE-Kriging is generally constructed in a constrained box space, and since physical parameter units should be normalized, it is recommended to scale the input parameter space to a hypercube $[0, 1]^n$. Consequently, the derivative-based

global sensitivity index can be estimated with the Monte Carlo method as

$$S_k \approx \hat{S}_k = \frac{1}{N} \sum_{i=1}^N \left(\frac{\partial g(\mathbf{x}^{(i)})}{\partial x_k} \right)^2, \quad (11)$$

where $\mathbf{x}^{(i)} (i = 1, \dots, N)$ are the observed sampling sites.

By ranking the input variables according to their sensitivity indices in descending order, the effective dimension n' of $g(\mathbf{x})$ can be determined from

$$\frac{\sum_{k=1}^{n'} \hat{S}_k}{\sum_{k=1}^n \hat{S}_k} > 1 - \epsilon, \quad (12)$$

where ϵ is a user-specified constant, e.g., $\epsilon = 0.01, 0.001$, etc.

After a low-dimensional subspace is detected, one can train the SGE-Kriging model with considering only the observed function values and the associated partial derivatives within the identified subspace [4, 5]. Consequently, the correlation matrix of SGE-Kriging is reduced from $N(n+1) \times N(n+1)$ to $N(n'+1) \times N(n'+1)$. Moreover, the sensitivity indices provide us with useful information for tuning the hyper-parameters $\boldsymbol{\theta} = [\theta_1, \dots, \theta_n]^T$. In fact, similar to the global sensitivity indices, the hyper-parameters θ_k , ($k = 1, \dots, n$) that measure the correlation lengths in the various coordinate directions, can be interpreted as measuring how strongly the corresponding input variable x_k , ($k = 1, \dots, n$) affects the response of a GE-Kriging model [4, 37]. For an input variable with large sensitivity index, one can deduce that the hyper-parameter of GE-Kriging model on the corresponding direction tends to be large, and vice versa [4, 37].

3.2. Sliced likelihood function

In this subsection, we will introduce the sliced likelihood function, based on which the correlation of the whole sample set can be described with multiple small matrices rather than a single big one.

In Fig. 1, a one-dimensional biquadratic spline correlation function as detailed in Eq. (A.1) is depicted. Obviously, along every direction $k = 1, \dots, n$, the sample correlation depends on the spatial distance $|x_k - \hat{x}_k|$ as well as on the value of the corresponding hyper-parameter θ_k . The sample correlation is weak when the spatial distance is large or when the hyper-parameter is large. Therefore, we propose to neglect the correlation between samples that are far away from each other along direction with the

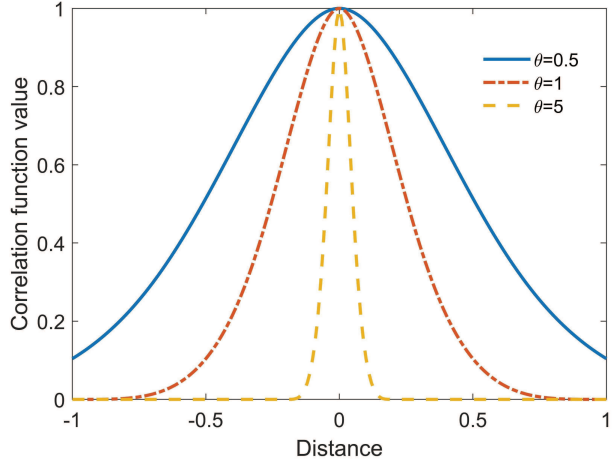


Figure 1: Biquadratic spline correlation function with different hyper-parameter θ .

largest hyper-parameter value. To this end, we divide the support $[0,1]$ of the most important input variable x_1 (the input variable ranked with the largest sensitivity index) into m successive and non-overlapping subintervals $\mathcal{A}_1 = [a_0, a_1], \dots, \mathcal{A}_m = [a_{m-1}, a_m]$, $a_0 = 0, a_m = 1$, and the hyper-cube $[0, 1]^n$ of the input parameter space is thus partitioned into m slices $\mathcal{D}_1 = [a_0, a_1] \times [0, 1]^{n-1}, \dots, \mathcal{D}_m = [a_{m-1}, a_m] \times [0, 1]^{n-1}$, as shown in Fig. 2. Consequently, the whole observed sample set (\mathbf{X}, \mathbf{y}) is correspondingly splitted into m non-overlapping subsets. Here we denote the subset of input sampling sites and corresponding model response within each slices \mathcal{D}_i as $\bar{\mathbf{X}}_i$ and $\bar{\mathbf{y}}_i$ respectively, thus we have $\mathbf{X} = \bar{\mathbf{X}}_1 \cup \bar{\mathbf{X}}_2 \cup \dots \cup \bar{\mathbf{X}}_m$, $\mathbf{y} = \bar{\mathbf{y}}_1 \cup \bar{\mathbf{y}}_2 \cup \dots \cup \bar{\mathbf{y}}_m$. Each subset contains N_i samples so that $(\sum_{i=1}^m N_i = N)$.

Note that above partition strategy should guarantee that the number of samples within each slice should be as balanced as possible. To achieve this goal, we rank the N samples of the most important input variable x_1 in index-ascending order as $x_1^{(1)}, \dots, x_1^{(N)}$, and set $a_i = (x_1^{(\sum_{j=1}^i N_j)} + x_1^{(\sum_{j=1}^i N_j + 1)})/2$, ($i = 1, \dots, m-1$), in which $N_i = \lfloor N/m \rfloor + 1$, ($i = 1, \dots, N_r$), $N_i = \lfloor N/m \rfloor$ ($i = N_r + 1, \dots, m$), and $N_r = N \bmod m$.

Using Bayes' theorem, the likelihood function of GE-Kriging can be rewritten as

$$f(\mathbf{y}) = f(\bar{\mathbf{y}}_1) f(\bar{\mathbf{y}}_2 | \bar{\mathbf{y}}_1) f(\bar{\mathbf{y}}_3 | \bar{\mathbf{y}}_1, \bar{\mathbf{y}}_2) \cdots f(\bar{\mathbf{y}}_m | \bar{\mathbf{y}}_1, \bar{\mathbf{y}}_2, \dots, \bar{\mathbf{y}}_{m-1}). \quad (13)$$

By assuming that the samples within non-adjacent slices are virtually

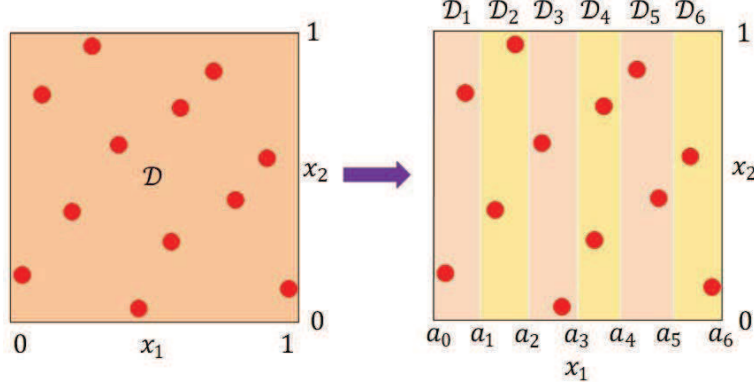


Figure 2: A two dimensional example of splitting the whole training sample set (left) into six slices (right) along the x_1 -coordinate direction

independent, we obtain the following approximated likelihood function $\hat{f}(\mathbf{y})$,

$$\begin{aligned}
 \hat{f}(\mathbf{y}) &= f(\bar{\mathbf{y}}_1)f(\bar{\mathbf{y}}_2|\bar{\mathbf{y}}_1)f(\bar{\mathbf{y}}_3|\bar{\mathbf{y}}_2)\cdots f(\bar{\mathbf{y}}_m|\bar{\mathbf{y}}_{m-1}) \\
 &= \frac{f(\bar{\mathbf{y}}_1, \bar{\mathbf{y}}_2)f(\bar{\mathbf{y}}_2, \bar{\mathbf{y}}_3)\cdots f(\bar{\mathbf{y}}_{m-1}, \bar{\mathbf{y}}_m)}{f(\bar{\mathbf{y}}_2)f(\bar{\mathbf{y}}_3)\cdots f(\bar{\mathbf{y}}_{m-1})} \\
 &= \frac{\prod_{i=1}^{m-1} f(\bar{\mathbf{y}}_i, \bar{\mathbf{y}}_{i+1})}{\prod_{i=2}^{m-1} f(\bar{\mathbf{y}}_i)}.
 \end{aligned} \tag{14}$$

Since in Eq. (14), the correlation between samples from two adjacent slices are considered, we call the approximated likelihood function $\hat{f}(\mathbf{y})$ the *2-appendant likelihood function*, and the corresponding GE-Kriging model by the name of *2-appendant SGE-Kriging*. Note that this approach can be readily extended to incorporate the correlation of data from more than two slices. For example, the 3-appendant likelihood function is defined as

$$\begin{aligned}
 \hat{f}(\mathbf{y}) &= f(\bar{\mathbf{y}}_1)f(\bar{\mathbf{y}}_2|\bar{\mathbf{y}}_1)f(\bar{\mathbf{y}}_3|\bar{\mathbf{y}}_1, \bar{\mathbf{y}}_2)f(\bar{\mathbf{y}}_4|\bar{\mathbf{y}}_2, \bar{\mathbf{y}}_3)\cdots f(\bar{\mathbf{y}}_m|\bar{\mathbf{y}}_{m-2}, \bar{\mathbf{y}}_{m-1}) \\
 &= \frac{f(\bar{\mathbf{y}}_1, \bar{\mathbf{y}}_2, \bar{\mathbf{y}}_3)f(\bar{\mathbf{y}}_2, \bar{\mathbf{y}}_3, \bar{\mathbf{y}}_4)\cdots f(\bar{\mathbf{y}}_{m-2}, \bar{\mathbf{y}}_{m-1}, \bar{\mathbf{y}}_m)}{f(\bar{\mathbf{y}}_2, \bar{\mathbf{y}}_3)f(\bar{\mathbf{y}}_3, \bar{\mathbf{y}}_4)\cdots f(\bar{\mathbf{y}}_{m-2}, \bar{\mathbf{y}}_{m-1})} \\
 &= \frac{\prod_{i=1}^{m-2} f(\bar{\mathbf{y}}_i, \bar{\mathbf{y}}_{i+1}, \bar{\mathbf{y}}_{i+2})}{\prod_{i=2}^{m-2} f(\bar{\mathbf{y}}_i, \bar{\mathbf{y}}_{i+1})}.
 \end{aligned} \tag{15}$$

In theory, the 3-appendant likelihood function is closer to the original likelihood function since more sample correlations are retained. It is therefore

expected to provide better approximations than the 2-appendant one from Eq. (14). However, according to our numerical experiments, the 2-appendant likelihood function already yields satisfactory approximation results for most tested problems, see the upcoming discussion in Section 4. Therefore, we proceed with the discussion of the 2-appendant likelihood function, and use this example to explain how to conduct the hyper-parameter tuning for SGE-Kriging.

Denoting $\bar{\mathbf{y}}_{2*i} = [\bar{\mathbf{y}}_i, \bar{\mathbf{y}}_{i+1}]^T$, we have

$$\begin{aligned} f(\bar{\mathbf{y}}_{2*i}) &= \frac{\exp\left(-\frac{1}{2\sigma^2}(\bar{\mathbf{y}}_{2*i} - \beta_0 \bar{\mathbf{F}}_{2*i})^T \bar{\mathbf{R}}_{2*i}^{-1}(\bar{\mathbf{y}}_{2*i} - \beta_0 \bar{\mathbf{F}}_{2*i})\right)}{\sqrt{(2\pi\sigma^2)^{N_{2*i}} [\det \bar{\mathbf{R}}_{2*i}]}} , \\ f(\bar{\mathbf{y}}_i) &= \frac{\exp\left(-\frac{1}{2\sigma^2}(\bar{\mathbf{y}}_i - \beta_0 \bar{\mathbf{F}}_i)^T \bar{\mathbf{R}}_{i,i}^{-1}(\bar{\mathbf{y}}_i - \beta_0 \bar{\mathbf{F}}_i)\right)}{\sqrt{(2\pi\sigma^2)^{\bar{N}_i} [\det \bar{\mathbf{R}}_{i,i}]}} , \end{aligned}$$

where

$$\begin{aligned} \bar{\mathbf{F}}_{2*i} &= [\underbrace{1, \dots, 1}_{N_i}, \underbrace{0, \dots, 0}_{n'N_i}, \underbrace{1, \dots, 1}_{N_{i+1}}, \underbrace{0, \dots, 0}_{n'N_{i+1}}]^T, \\ \bar{\mathbf{F}}_i &= [\underbrace{1, \dots, 1}_{N_i}, \underbrace{0, \dots, 0}_{n'N_i}]^T, \end{aligned}$$

and the dimensions are $\bar{N}_{2*i} = (N_i + N_{i+1})(n' + 1)$, and $\bar{N}_i = N_i(n' + 1)$. The reduced correlation matrix is

$$\bar{\mathbf{R}}_{2*i} = \begin{bmatrix} \bar{\mathbf{R}}_{i,i} & \bar{\mathbf{R}}_{i,i+1} \\ \bar{\mathbf{R}}_{i,i+1}^T & \bar{\mathbf{R}}_{i+1,i+1} \end{bmatrix} \in \mathbb{R}^{\bar{N}_{2*i} \times \bar{N}_{2*i}}.$$

Here, the sub-block $\bar{\mathbf{R}}_{i_1, i_2}$ represents the correlation matrix of $\bar{\mathbf{y}}_{i_1}$ and $\bar{\mathbf{y}}_{i_2}$, namely,

$$\bar{\mathbf{R}}_{i_1, i_2} = \begin{bmatrix} \mathbf{R}_{i_1, i_2} & \partial \mathbf{R}_{i_1, i_2} \\ \partial \mathbf{R}_{i_1, i_2}^T & \partial^2 \mathbf{R}_{i_1, i_2} \end{bmatrix} \in \mathbb{R}^{\bar{N}_{i_1} \times \bar{N}_{i_2}},$$

and its elements are given by

$$\begin{aligned} (\mathbf{R}_{i_1, i_2})_{k_1, k_2} &:= R(\mathbf{x}^{(k_1)}, \mathbf{x}^{(k_2)}; \boldsymbol{\theta}), \\ (\partial \mathbf{R}_{i_1, i_2})_{k_1, k_2} &:= \frac{\partial R(\mathbf{x}^{(k_1)}, \mathbf{x}^{(k_2)}; \boldsymbol{\theta})}{\partial x_{l_1}^{(k_2)}}, l_1 = 1, \dots, n' \\ (\partial^2 \mathbf{R}_{i_1, i_2})_{k_1, k_2} &:= \frac{\partial^2 R(\mathbf{x}^{(k_1)}, \mathbf{x}^{(k_2)}; \boldsymbol{\theta})}{\partial x_{l_1}^{(k_1)} \partial x_{l_2}^{(k_2)}}, l_1, l_2 = 1, \dots, n'. \end{aligned}$$

where $k_1 = \sum_{j=1}^{i_1-1} N_j + 1, \dots, \sum_{j=1}^{i_1} N_j$, $k_2 = \sum_{j=1}^{i_2-1} N_j + 1, \dots, \sum_{j=1}^{i_2} N_j$.

Taking logarithm of $\hat{f}(\mathbf{y})$ from Eq. (14), we have

$$\ln \hat{f}(\mathbf{y}) = \sum_{i=1}^{m-1} \ln f(\bar{\mathbf{y}}_i, \bar{\mathbf{y}}_{i+1}) - \sum_{i=2}^{m-1} \ln f(\bar{\mathbf{y}}_i). \quad (16)$$

Considering the hyper-parameters $\boldsymbol{\theta}$ as fixed and setting the partial derivatives of $\ln \hat{f}(\mathbf{y})$ with respect to β_0 and σ^2 to zero, we obtain their optimal values analytically as

$$\begin{aligned} \beta_0 &= \left(\sum_{i=1}^{m-1} \bar{\mathbf{F}}_{2*i}^T \bar{\mathbf{R}}_{2*i}^{-1} \bar{\mathbf{F}}_{2*i} - \sum_{i=2}^{m-1} \bar{\mathbf{F}}_i^T \bar{\mathbf{R}}_{i,i}^{-1} \bar{\mathbf{F}}_i \right)^{-1} \\ &\quad \left(\sum_{i=1}^{m-1} \bar{\mathbf{F}}_{2*i}^T \bar{\mathbf{R}}_{2*i}^{-1} \bar{\mathbf{y}}_{2*i} - \sum_{i=2}^{m-1} \bar{\mathbf{F}}_i^T \bar{\mathbf{R}}_{i,i}^{-1} \bar{\mathbf{y}}_i \right), \\ \sigma^2 &= \frac{1}{(n'+1)N} \left(\sum_{i=1}^{m-1} (\bar{\mathbf{y}}_{2*i} - \beta_0 \bar{\mathbf{F}}_{2*i})^T \bar{\mathbf{R}}_{2*i}^{-1} (\bar{\mathbf{y}}_{2*i} - \beta_0 \bar{\mathbf{F}}_{2*i}) - \right. \\ &\quad \left. \sum_{i=2}^{m-1} (\bar{\mathbf{y}}_i - \beta_0 \bar{\mathbf{F}}_i)^T \bar{\mathbf{R}}_{i,i}^{-1} (\bar{\mathbf{y}}_i - \beta_0 \bar{\mathbf{F}}_i) \right). \end{aligned}$$

Note that the optimal values of β_0 and σ^2 still depend on the hyper-parameters $\boldsymbol{\theta}$. Inserting their optimal values into Eq. (16), we arrive at minimizing the following likelihood function

$$\ell(\boldsymbol{\theta}) = (n'+1)N \ln \sigma^2(\boldsymbol{\theta}) + \sum_{i=1}^{m-1} \ln [\det \bar{\mathbf{R}}_{2*i}(\boldsymbol{\theta})] - \sum_{i=2}^{m-1} \ln [\det \bar{\mathbf{R}}_{i,i}(\boldsymbol{\theta})]. \quad (17)$$

To evaluate this new likelihood function, the associated computational cost for decomposing $\bar{\mathbf{R}}_{2*i}$ ($i = 1, \dots, m-1$) and $\bar{\mathbf{R}}_{i,i}$ ($i = 2, \dots, m-1$) using the Cholesky method is $\mathcal{O}((m-1)(2n'+2)^3 N^3 / m^3 + (m-2)(n'+1)^3 N^3 / m^3)$. Therefore, the computational cost ratio for decomposing the correlation matrices of GE-Kriging and SGE-Kriging using the Cholesky method is given by

$$\frac{(n+1)^3 N^3}{(m-1)(2n'+2)^3 N^3 / m^3 + (m-2)(n'+1)^3 N^3 / m^3}, \quad (18)$$

In Table 1, the computational cost ratio in Eq. (18) with different settings are listed. It shows that the computational cost of SGE-Kriging is much lower

than that of GE-Kriging for various cases, especially for problems with small effective dimension n' and large slice number m .

Table 1: Comparison of cost ratios for computing the Cholesky decompositions for the correlation matrices in GE-Kriging and SGE-Kriging with different settings.

Dimension n	Dimension n'	Slice number m	Computational cost ratio
50	50	10	12.50
50	40	10	24.06
50	40	20	90.57
50	30	20	209.39
100	100	10	12.50
100	80	10	24.23
100	80	20	91.23
100	60	20	213.61

3.3. Hyper-parameter tuning

For high-dimensional problems, it is still challenging to tune the hyper-parameters $\boldsymbol{\theta} = [\theta_1, \dots, \theta_n]$ of SGE-Kriging by minimizing the likelihood function in Eq. (17). In this subsection, we will utilize the global sensitivity analysis results to reduce the number of hyper-parameters $\boldsymbol{\theta}$.

As mentioned earlier, the underlying meaning of the hyper-parameters θ_k , $(k = 1, \dots, n)$ for a GE-Kriging model is related with the global sensitivity indices S_k , $(k = 1, \dots, n)$ for a computational model $g(\mathbf{x})$. Therefore, this suggests a way to determine the hyper-parameters by exploring their relationship with the global sensitivity indices. However, a quantitative relationship cannot be obtained analytically. Therefore, we model the functional relationship via the following parameterized equation

$$\theta_k = \alpha_1 \hat{s}_k^{\alpha_2} + \alpha_3, \quad k = 1, \dots, n, \quad (19)$$

where \hat{s}_k represents the normalized sensitivity index, namely, $\hat{s}_k = \hat{S}_k / \sum_{l=1}^n (\hat{S}_l)$. Note that in this way all hyper-parameters θ_k are determined by the same three parameters $\alpha_1, \alpha_2, \alpha_3$ and the associated sensitivity index.

Consequently, the original many-parameter likelihood function is replaced with a 3-dimensional counterpart

$$\ell(\boldsymbol{\alpha}) = (n' + 1)N \ln \sigma^2(\boldsymbol{\alpha}) + \sum_{i=1}^{m-1} \ln [\det \bar{\mathbf{R}}_{2*i}(\boldsymbol{\alpha})] - \sum_{i=2}^{m-1} \ln [\det \bar{\mathbf{R}}_{i,i}(\boldsymbol{\alpha})] \quad (20)$$

where $\boldsymbol{\alpha} = [\alpha_1, \alpha_2, \alpha_3]^T$ is the vector of auxiliary parameters. After optimal $\boldsymbol{\alpha}$ are found by minimizing the likelihood function in Eq. (20) with a numerical optimization method, the hyper-parameters $\boldsymbol{\theta}$ are obtained according to Eq. (19).

When the hyper-parameters $\boldsymbol{\theta}$ of SGE-Kriging are determined, the final predictor of SGE-Kriging is consistent with the standard GE-Kriging in form, as presented in Eqs. (2)-(4), in which β_0 and σ^2 are given by Eqs. (6) and (7). However, one should note that we need to invert the correlation matrix $\mathbf{R} \in \mathbb{R}^{N(n'+1) \times N(n'+1)}$ with the Cholesky method one more time to eventually make predictions.

4. Numerical examples

In this section, we will demonstrate the effectiveness of SGE-Kriging on several benchmark problems, and its performance is compared to the standard GE-Kriging and Kriging without incorporating derivative data. The relative mean squared error (RMSE) is used to measure the accuracy of various surrogate models, which is defined as

$$\text{RMSE} = \frac{\sum_{i=1}^{N_1} (g(\mathbf{x}^{(i)}) - \mu(\mathbf{x}^{(i)}))^2}{\sum_{i=1}^{N_1} (g(\mathbf{x}^{(i)}) - \bar{g})^2}, \quad (21)$$

where $g(\mathbf{x}^{(i)})$ and $\mu(\mathbf{x}^{(i)})$, ($i = 1, \dots, N_1$) are the model response and the prediction of the surrogate model under consideration on the test sample points, respectively, and \bar{g} is the mean of the test sample response. In the experiments, we use $N_1 = 3000$.

As announced earlier, we scale the input space to a hypercube $[0, 1]^n$, and the gradient-free “Hooke&Jeeves” pattern search method [18] with 10 random starts is used to optimize the hyper-parameters of the various surrogate models. For standard GE-Kriging and the Kriging model, the hyper-parameters θ_k , ($k = 1, \dots, n$) are confined to the range of $[0.0005, 5]$. In SGE-Kriging, the auxiliary parameters α_1 , α_2 and α_3 are limited to intervals $[0.0005, 2.5]$, $[0.2, 1]$ and $[0.0005, 2.5]$, respectively, such that the hyper-parameter θ_k , ($k = 1, \dots, n$) of SGE-Kriging shares the same bound with that of GE-Kriging.

4.1. One-dimensional example

In this subsection, the following one-dimensional analytical function is used to illustrate the effectiveness of SGE-Kriging

$$g(\mathbf{x}) = e^{-x} + \sin(5x) + \cos(5x) + 0.2x + 4, x \in [0, 6]. \quad (22)$$

We generate 10 samples with the Latin Hypercubic Sampling (LHS) method and construct GE-Kriging and SGE-Kriging predictors using the cubic and the biquadratic spline correlation functions. In SGE-Kriging, the sample set is divided into $m = 5$ and $m = 10$ slices equally, and the sliced likelihood functions are depicted in Figs. 3 and 4, respectively for comparison.

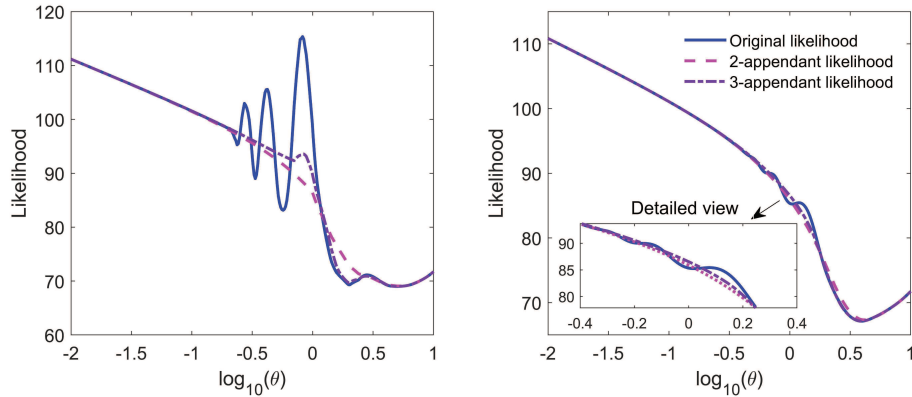


Figure 3: Comparison of likelihood functions of GE-Kriging and SGE-Kriging with $m = 5$ using cubic spline correlation function (left) and biquadratic spline correlation function (right) for Example 4.1

For standard GE-Kriging, it is observed that the cubic spline function yields a likelihood function that exhibits a much more complex behavior with many local minima when compared to the biquadratic one, which suggests that the biquadratic spline function is more benign than the cubic spline one for applications in GE-Kriging. In contrast, the likelihood functions of SGE-Kriging exhibit a simpler shape when compared to the original one for both the two correlation functions with various settings, but they still feature the optimal value of the model hyper-parameter at virtually the same location. Additionally, as expected from the theory, the example shows that the likelihood functions of SGE-Kriging with less slices ($m = 5$) or with

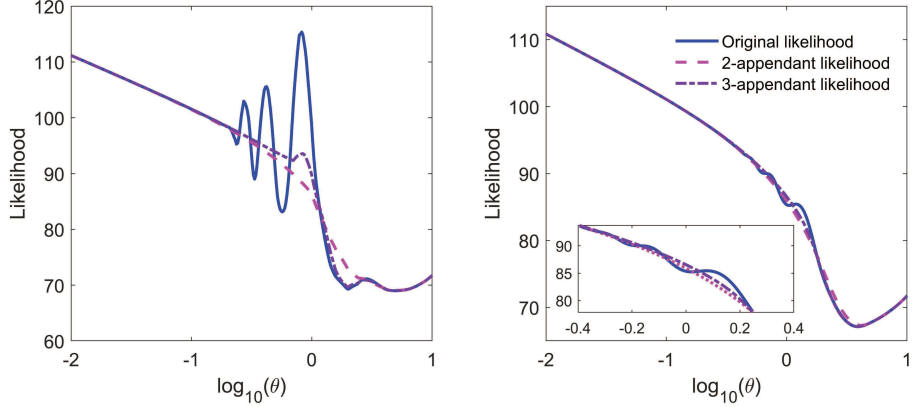


Figure 4: Comparison of likelihood functions of GE-Kriging and SGE-Kriging with $m = 10$ for Example 4.1 using the cubic spline correlation function (left) and the biquadratic spline correlation function (right)

considering the correlation of samples within more adjacent slices yield better approximations of the original likelihood function. Also, one can see that the 2-appendant likelihood function of SGE-Kriging with $m = 10$ already provides satisfactory results, and the improvement of 3-appendant likelihood function is marginal in this example, especially when the biquadratic spline function is used.

The prediction accuracy of Kriging, GE-Kriging and SGE-Kriging with $m = 10$ is depicted in Figs. 5 and 6 for comparison, and the detailed MSEs of various surrogate models are listed in Table 2. Note that for this one-

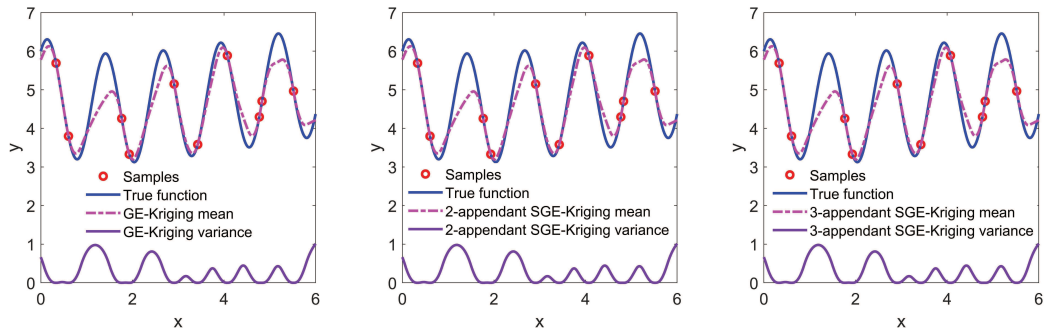


Figure 5: Comparisons of GE-Kriging and SGE-Kriging with $m = 10$ using the cubic spline correlation function for Example 4.1

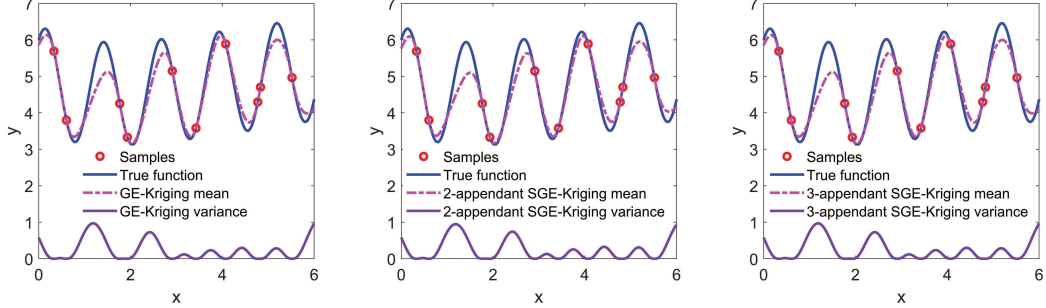


Figure 6: Comparison of GE-Kriging and SGE-Kriging with $m = 10$ using biquadratic spline correlation function for Example 4.1

dimensional problem, the single hyper-parameter θ of SGE-Kriging is determined by minimizing the likelihood function in Eq. (17) directly, i, e., without using the α -reparameterization in Eq. (19).

As expected, SGE-Kriging and GE-Kriging yield very similar predictions for both of the two correlation functions. Additionally, one can see that the GE-Kriging and SGE-Kriging predictors based on biquadratic spline correlation provide better results than the predictor that utilizes the cubic one, which confirms that the biquadratic spline function is superior to the cubic one for applications in GE-Kriging and SGE-Kriging.

Table 2: Comparison of optimal hyper-parameters (obtained by grid search) and MSEs of GE-Kriging and SGE-Kriging with $m = 10$ using different correlation functions for Example 4.1.

Surrogate model	correlation function	Optimal θ	MSE
GE-Kriging	cubic spline	3.7896	0.1263
GE-Kriging	biquadratic spline	3.9688	0.0875
2-appendant SGE-Kriging	cubic spline	3.7031	0.1230
2-appendant SGE-Kriging	biquadratic spline	4.1565	0.0956
3-appendant SGE-Kriging	cubic spline	3.7031	0.1272
3-appendant SGE-Kriging	biquadratic spline	3.9688	0.0875

4.2. Two-dimensional example

In this subsection, a two-dimensional analytical function is used to demonstrate the effectiveness of the proposed SGE-Kriging model. The test

function is defined as

$$g(\mathbf{x}) = (4 - 2.1x_1^2 + \frac{x_1^4}{3})x_1^2 + x_1x_2 + (4x_2^2 - 4)x_2^2, \quad (23)$$

where $x_1 \in [-2, 2]$ and $x_2 \in [-1, 1]$.

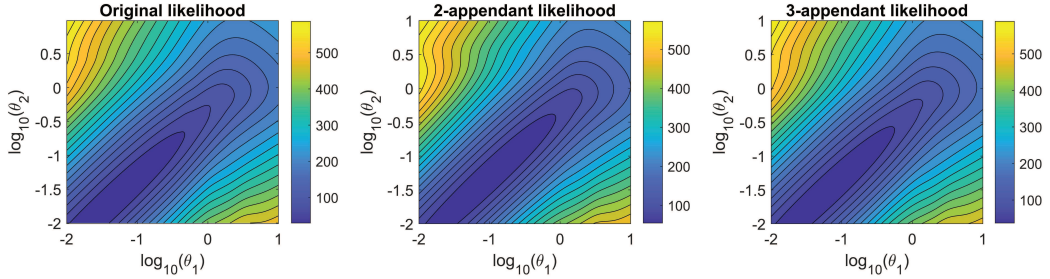


Figure 7: (cf. Example 4.2) Comparison of the likelihood functions of GE-Kriging (left) and SGE-Kriging (middle, right) based on the biquadratic spline correlation function with $m = 5$.

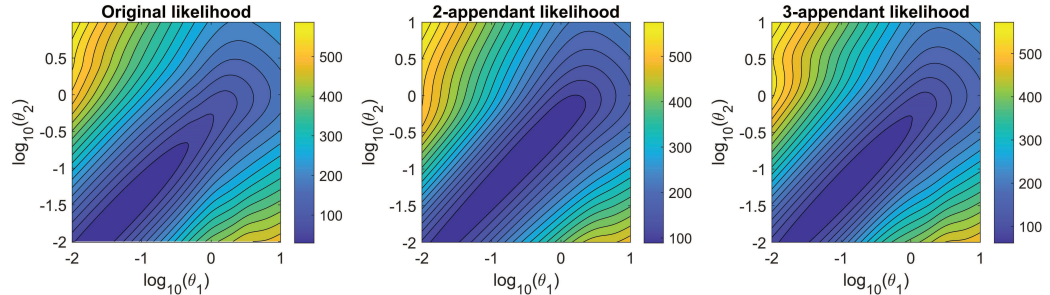


Figure 8: (cf. Example 4.2) Same as Figure 7 but with SGE-Kriging with $m = 10$.

In this example, 20 samples generated with LHS randomly are used to train the various surrogate models. The likelihood functions of GE-Kriging and SGE-Kriging with different settings are depicted in Figs. 7–9. It can be seen that the likelihood functions of SGE-Kriging mimics the global behavior of the original one quite well in all the considered cases. In Table 3, the optimal hyper-parameters suggested by different likelihood functions and the corresponding minimal likelihood function values are listed. Again, we see that the likelihood functions of SGE-Kriging with less slices or with considering the correlation of samples within more adjacent slices yield better approximations of the original one.

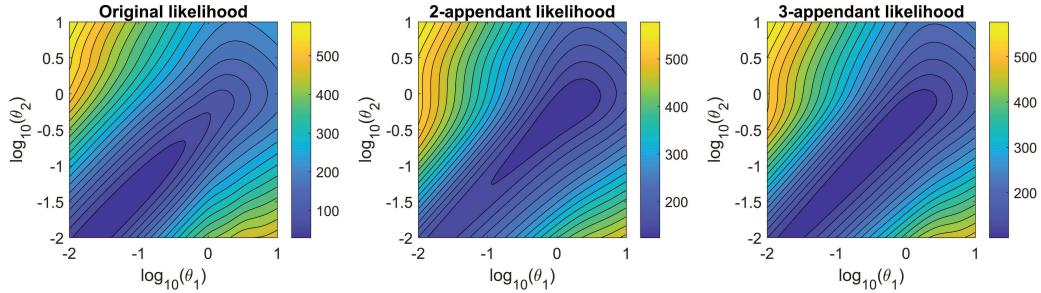


Figure 9: (cf. Example 4.2) Same as Figure 7 but with SGE-Kriging with $m = 20$.

Table 3: Comparison of optimal hyper-parameters (obtained by grid search) and minimal likelihood function values of GE-Kriging and SGE-Kriging with different settings for Example 4.2.

Likelihood function	θ_1	θ_2	Likelihood value
Original likelihood	0.0445	0.0222	28.9504
2-appendant likelihood ($m = 5$)	0.0988	0.0477	42.1823
2-appendant likelihood ($m = 10$)	0.5053	0.2613	87.7040
2-appendant likelihood ($m = 20$)	0.9437	0.4103	104.3997
3-appendant likelihood ($m = 5$)	0.0548	0.0273	31.4144
3-appendant likelihood ($m = 10$)	0.1499	0.0749	58.9102
3-appendant likelihood ($m = 20$)	0.6905	0.3449	97.1606

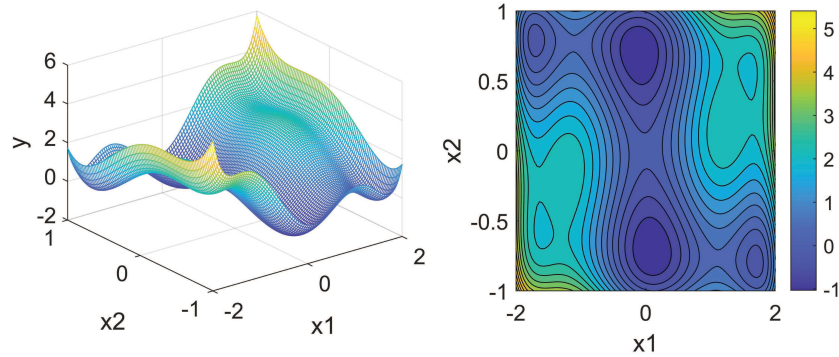


Figure 10: (cf. Example 4.2) True response surface (left) and contour plot (right).

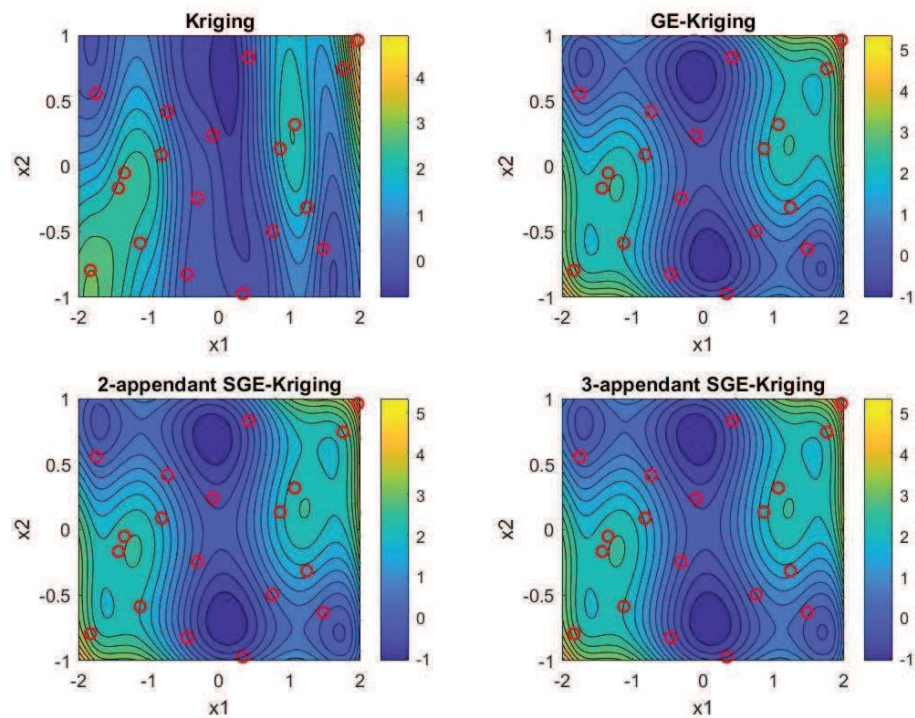


Figure 11: (cf. Example 4.2) Comparison of the prediction mean of Kriging, GE-Kriging and SGE-Kriging with $m = 10$ using the biquadratic spline correlation function.

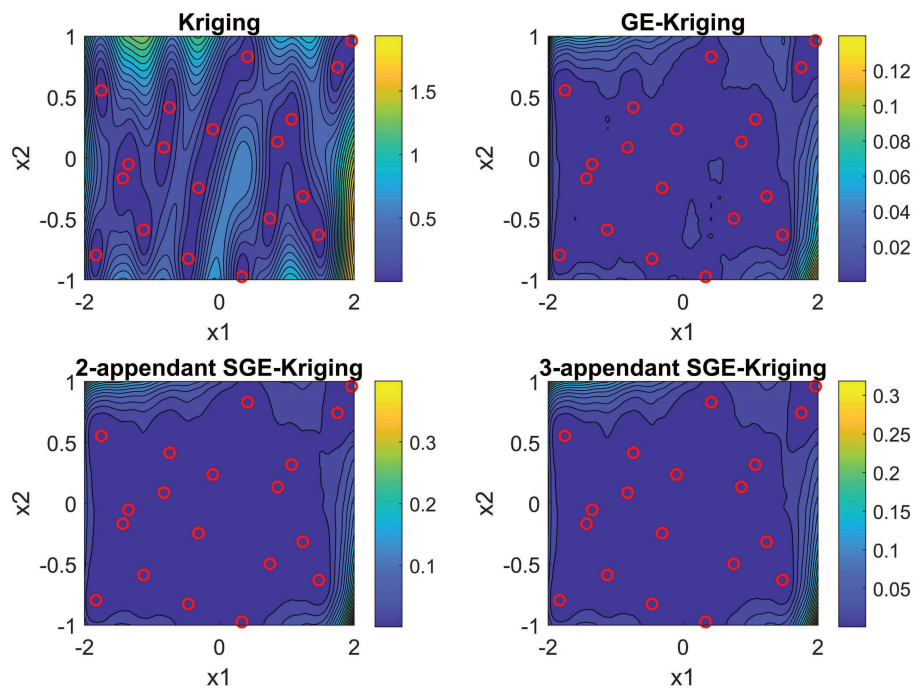


Figure 12: (cf. Example 4.2) Comparison of the prediction variance of Kriging, GE-Kriging and SGE-Kriging with $m = 10$ using the biquadratic spline correlation function.

The true response surface of this function and the corresponding contour are shown in Fig. 10, and the performance of Kriging, GE-Kriging and SGE-Kriging with 10 total slices is depicted in Fig. 11. For this two-dimensional problem, the hyper-parameters of SGE-Kriging are still tuned by minimizing the likelihood function in Eq. (17) without using the α -reparameterization in Eq. (19). It shows that SGE-Kriging and GE-Kriging provide similar predictions, and both of them outperform Kriging significantly. Specifically, the MSEs of Kriging, GE-Kriging, 2-appendant and 3-appendant SGE-Kriging are 0.1140, 0.00175, 0.00306 and 0.00212, respectively, which conforms the effectiveness of SGE-Kriging. Moreover, in Fig. 12, we see that the prediction variance of SGE-Kriging is slightly higher than that of GE-Kriging. Indeed, since part of the sample correlation is neglected, the accuracy of SGE-Kriging is expected to be inferior to GE-Kriging in theory.

4.3. High-dimensional Dixon-Price test function

In this subsection, we demonstrate the performance of SGE-Kriging on a high-dimensional Dixon-Price function [37], which is defined as

$$g(\mathbf{x}) = (x_1 - 1)^2 + \sum_{i=2}^n i(2x_i^2 - x_{i-1})^2, x_i \in [-10, 10], (i = 1, \dots, n). \quad (24)$$

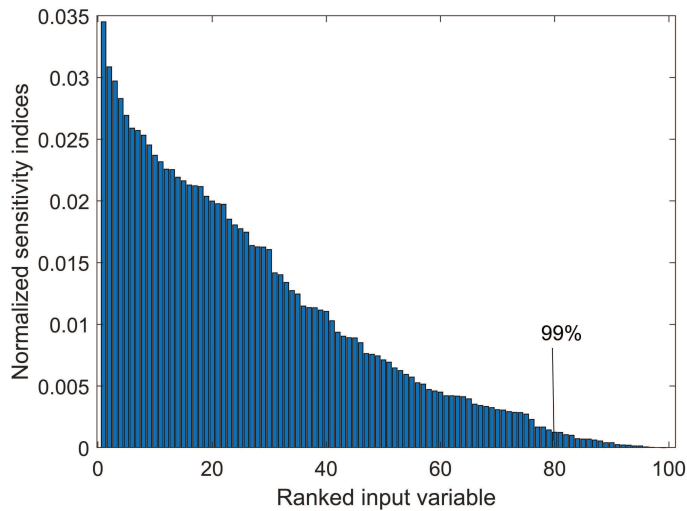


Figure 13: (cf. Example 4.3) Global sensitivity analysis result (with 100 sampling sites) for a 100-dimensional Dixon-Price function.

We set the input dimension to $n = 50$ and $n = 100$ respectively. To construct the SGE-Kriging predictor, the derivative-based global sensitivity analysis method introduced in Section 3.1 is used to detect the effective parameter dimension of the Dixon-Price function. Here we set the threshold in Eq. (12) to $\epsilon = 0$ and $\epsilon = 0.01$ respectively. For the first case, all the gradient information is utilized to train SGE-Kriging, and the effective parameter dimension of the Dixon-Price function is $n' = n$. For the second case, 99% of the gradient information contents is retained in SGE-Kriging, and the effective parameter dimension of the 100-Dixon-Price function is about $n' = 80$, as depicted in Fig. 13, which allows us to reduce the correlation matrix size of the whole sample set by about $1 - (n' + 1)^2 / (n + 1)^2 = 35.7\%$. Additionally, the hyper-parameter tuning method presented in Section 3.3 is used to determine the high-dimensional hyper-parameters of the SGE-Kriging model.

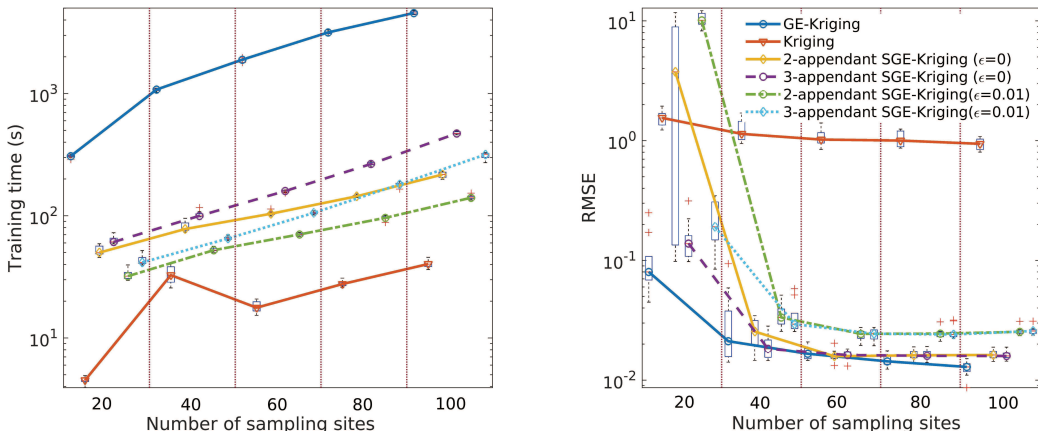


Figure 14: (cf. Example 4.3) Comparison of the performance of Kriging, GE-Kriging and SGE-Kriging with $m = 10$ and $\epsilon = 0$ using the biquadratic spline correlation function for a 50-dimensional Dixon-Price test function. Left: training time versus number of sample sites. Right: RMSE according to Eq. (21) versus number of sample site.

The RMSEs and training times of GE-Kriging, SGE-Kriging and Kriging versus the number of sampling sites are depicted in Figs. 14-15. Note that here, all the calculations are repeated 10 times to level out the effects of randomness in the training sample set, and all the numerical experiments are performed on the same HPC-cluster on the UCloud platform (Inter Xeon Gold 6130 CPU, 64-cores, 2.1GHz).

Here, the box plots are provided to illustrate the robustness of the different methods. In these plots, the central mark of each box indicates the

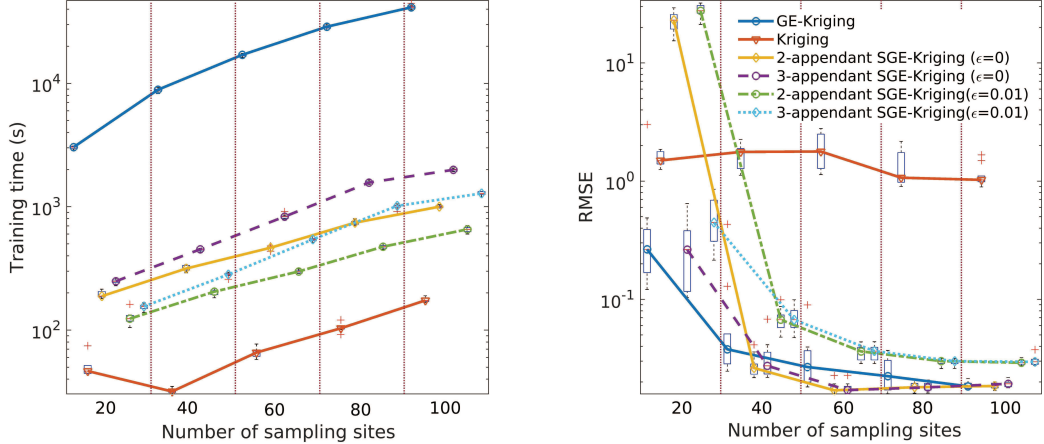


Figure 15: (cf. Example 4.3) Same as Fig. 14, but for a 100-dimensional Dixon-Price function.

median, and the bottom and top edges of the box indicate the 25th and 75th percentiles, and outliers are plotted individually using the '+' marker. For $\epsilon = 0$, it shows that the accuracy of SGE-Kriging is comparable to GE-Kriging for both 50 and 100-dimensional Dixon-Price function. Due to part of the gradient information being abandoned, the training efficiency of SGE-Kriging with $\epsilon = 0.01$ is improved to some degree, but its accuracy is slightly reduced compared to SGE-Kriging with $\epsilon = 0$. In addition, one can see that train a GE-Kriging model is quite time-consuming. It takes more than 4500s and 40000s to train a GE-Kriging model for a 50 and a 100-dimensional Dixon-Price function with 100 sampling sites, respectively. Compared to GE-Kriging, the training time of SGE-Kriging is reduced sharply. Specifically, using 100 sample points, training a 2-appendant SGE-Kriging with $\epsilon = 0(0.01)$ is 20(30) and 40(60) times faster than GE-Kriging for a 50 and a 100-dimensional Dixon-Price function, respectively.

Additionally, it shows that SGE-Kriging exhibits a bad approximation quality, when the total number of sampling sites is small. In these cases, the sampling sites within each slice is too small, and the sliced likelihood function cannot approximate the original one very well. However, the performance improves considerably with increasing the number of sampling sites. Compared to the 2-appendant SGE-Kriging, the training time of the 3-appendant SGE-Kriging rises slightly, and the model accuracy is comparable with the 2-appendant one.

4.4. 100-dimensional modified Rosenbrock function

In this subsection, a modified high-dimensional Rosenbrock function [37], is employed to further demonstrate the performance of SGE-Kriging. The test function is

$$g(\mathbf{x}) = \sum_{i=1}^{n-1} (x_i - 1)^4 + \sum_{i=2}^n \sqrt{i} (x_i - x_{i-1}^2)^2, x_i \in [-10, 10], (i = 1, \dots, n) \quad (25)$$

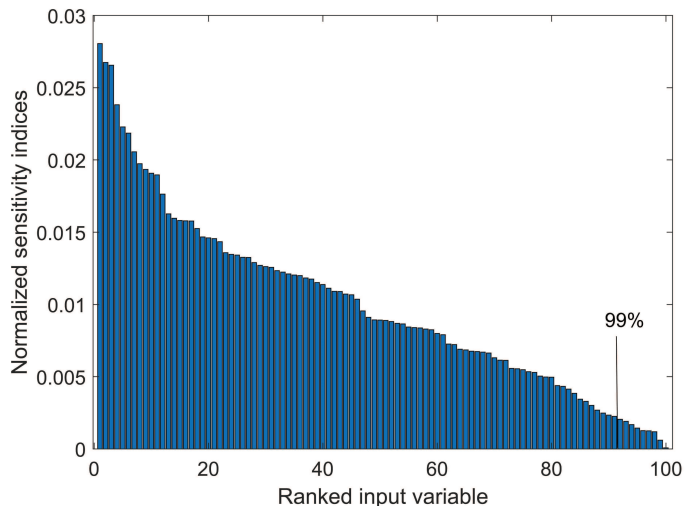


Figure 16: (cf. Example 4.4) Global sensitivity analysis result (with 100 sampling sites) for a 100-dimensional modified Rosenbrock test function

In this example, the input dimension is set as $n = 100$, and we train various surrogate models with the same settings as in Example 4.3. Here we again set the threshold in Eq. (12) to $\epsilon = 0$ and $\epsilon = 0.01$ respectively, and the derivative-based global sensitivity analysis results for the 100-dimensional modified Rosenbrock function are depicted in Fig. 16. One can see that the effective dimension of the modified Rosenbrock function function is about $n' = 92$ for $\epsilon = 0.01$, which corresponds to a relative gradient information content of $\approx 99\%$.

The RMSEs and training times of GE-Kriging, SGE-Kriging and Kriging versus the number of sampling sites are depicted in Fig. 17. In this example, it shows that SGE-Kriging with $\epsilon = 0$ outperforms other methods when the number of sampling sites is small. With the increase of sampling sites, GE-Kriging still yield the most accurate predictor. Again, the accuracy of

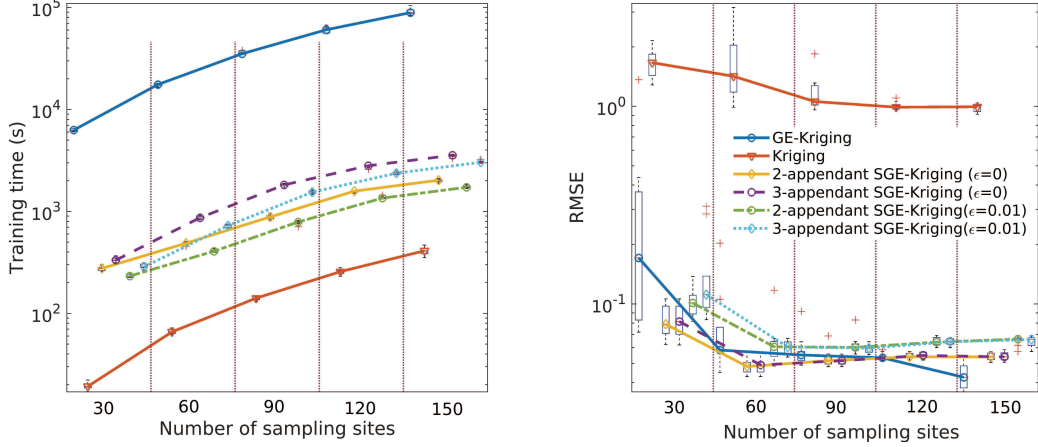


Figure 17: (cf. Example 4.4) Comparison of the performance of Kriging, GE-Kriging and SGE-Kriging with $m = 10$ using biquadratic spline correlation function for 100-dimensional modified Rosenbrock function

SGE-Kriging with $\epsilon = 0.01$ is slightly degenerated compared to SGE-Kriging with $\epsilon = 0$, but its training efficiency is improved to some degree.

In GE-Kriging, it takes about 8.8×10^4 s ($\approx 24.5h$, i.e., more than one day!) to train a GE-Kriging model for a 100-dimensional modified Rosenbrock function with 150 sampling sites. In contrast, with the same sampling sites, training a 2-appendant SGE-Kriging with $\epsilon = 0(0.01)$ is about 40(50) times faster than training GE-Kriging for a 100-dimensional modified Rosenbrock function. This example demonstrates again that SGE-Kriging provides a satisfactory balance between accuracy and efficiency.

5. Conclusions

In this paper, we have proposed a novel variant of GE-Kriging, termed sliced gradient-enhanced Kriging (SGE-Kriging), with the designated goal to increase the efficiency for constructing high-dimensional surrogate models that incorporate gradient information. The contribution of this work is twofold. First, by splitting the sampling sites into multiple non-overlapping slices, we propose a family of approximate ‘‘sliced’’ likelihood functions based on Bayes’ theorem. In this family, we neglect the correlation between data samples from slices that are far away from each other. This allows us to describe the correlation of the whole training sample set with multiple small

correlation matrices rather than a single big one. Second, we propose a parameterized equation to learn the relationship between the derivative-based global sensitivity indices and the hyper-parameters of SGE-Kriging. The original high-dimensional hyper-parameter optimization problem is thus replaced with a 3-dimensional counterpart.

The validity of the sliced likelihood function is demonstrated with two visualized test functions. The results show that the sliced likelihood function yields a satisfactory approximation of the true one. It is generally observed to feature fewer local minima, but yet it gives optimal or near optimal hyper-parameter values. The performance of SGE-Kriging is also tested with two high-dimensional examples. The results shows that the accuracy of SGE-Kriging is comparable to GE-Kriging, but its training efficiency is improved by one to two orders of magnitude.

To guarantee the robustness of SGE-Kriging, one should split the sample set properly such that the number of sampling sites within each slice is not too small. However, we remark that the optimal number of slices m is a problem-dependent parameter, and our numerical experiment suggests that $m = 10$ is a good option. In the future, it is planned to apply the newly developed SGE-Kriging model to a high-dimensional design optimization problem.

6. Acknowledgement

This work is supported by the Austrian Research Promotion Agency FFG under the e!MISSION programme, project “InduHeat”, project number 881147.

Appendix A. The biquadratic spline correlation function

With $\xi = \xi(|x - \hat{x}|; \theta) := \theta|x - \hat{x}|$, the biquadratic spline correlation function is defined as

$$R(|x - \hat{x}|; \theta) = \begin{cases} 1 - 15\xi^2 + 35\xi^3 - \frac{195}{8}\xi^4, & 0 \leq \xi < 0.4, \\ \frac{5}{3} - \frac{20}{3}\xi + 10\xi^2 - \frac{20}{3}\xi^3 + \frac{5}{3}\xi^4, & 0.4 \leq \xi < 1, \\ 0, & 1 \leq \xi. \end{cases} \quad (\text{A.1})$$

The first-order partial derivative of the biquadratic spline correlation function is

$$\frac{\partial R(\mathbf{x}, \hat{\mathbf{x}}; \boldsymbol{\theta})}{\partial x_k} = \frac{\partial R(|x_k - \hat{x}_k|; \theta_k)}{\partial x_k} \prod_{i=1, i \neq k}^n R(|x_i - \hat{x}_i|; \theta_i),$$

where

$$\frac{\partial R(|x - \hat{x}|; \theta)}{\partial x} = \begin{cases} \left(-30\xi + 105\xi^2 - \frac{195}{2}\xi^3\right) \theta \text{sign}|x - \hat{x}|, & 0 \leq \xi < 0.4, \\ \left(-\frac{20}{3} + 20\xi - 20\xi^2 + \frac{20}{3}\xi^3\right) \theta \text{sign}|x - \hat{x}|, & 0.4 \leq \xi < 1, \\ 0, & 1 \leq \xi. \end{cases}$$

Similarly, the second-order partial derivative of the biquadratic spline correlation function are

$$\frac{\partial^2 R(\mathbf{x}, \hat{\mathbf{x}}; \theta)}{\partial x_k \partial \hat{x}_l} = \begin{cases} \frac{\partial^2 R(|x_k - \hat{x}_k|; \theta_k)}{\partial x_k \partial \hat{x}_k} \prod_{i=1, i \neq k}^n R(|x_i - \hat{x}_i|; \theta_i), & k = l, \\ -\frac{R(|x_k - \hat{x}_k|; \theta_k)}{\partial x_k} \frac{R(|x_l - \hat{x}_l|; \theta_l)}{\partial \hat{x}_l} \prod_{i=1, i \neq k, l}^n R(|x_i - \hat{x}_i|; \theta_i), & k \neq l. \end{cases}$$

where

$$\frac{\partial^2 R(|x - \hat{x}|; \theta)}{\partial x \partial \hat{x}} = \begin{cases} -\left(-30 + 210\xi - \frac{585}{2}\xi^2\right) \theta^2, & 0 \leq \xi < 0.4, \\ -(20 - 40\xi + 20\xi^2) \theta^2, & 0.4 \leq \xi < 1, \\ 0, & 1 \leq \xi. \end{cases}$$

References

- [1] Oludare Isaac Abiodun, Aman Jantan, Abiodun Esther Omolara, Kemi Victoria Dada, Nachaat AbdElatif Mohamed, and Humaira Arshad. State-of-the-art in artificial neural network applications: A survey. *Helijon*, 4(11):e00938, 2018.
- [2] W Kyle Anderson and V Venkatakrishnan. Aerodynamic design optimization on unstructured grids with a continuous adjoint formulation. *Computers & Fluids*, 28(4-5):443–480, 1999.
- [3] Géraud Blatman and Bruno Sudret. Adaptive sparse polynomial chaos expansion based on least angle regression. *Journal of computational Physics*, 230(6):2345–2367, 2011.
- [4] Mohamed A Bouhlel and Joaquim RRA Martins. Gradient-enhanced kriging for high-dimensional problems. *Engineering with Computers*, 35(1):157–173, 2019.
- [5] Liming Chen, Haobo Qiu, Liang Gao, Chen Jiang, and Zan Yang. A screening-based gradient-enhanced kriging modeling method for high-dimensional problems. *Applied Mathematical Modelling*, 69:15–31, 2019.

- [6] Liming Chen, Haobo Qiu, Liang Gao, Chen Jiang, and Zan Yang. Optimization of expensive black-box problems via gradient-enhanced kriging. *Computer Methods in Applied Mechanics and Engineering*, 362:112861, 2020.
- [7] Kai Cheng and Zhenzhou Lu. Adaptive sparse polynomial chaos expansions for global sensitivity analysis based on support vector regression. *Computers & Structures*, 194:86–96, 2018.
- [8] Kai Cheng and Zhenzhou Lu. Adaptive bayesian support vector regression model for structural reliability analysis. *Reliability Engineering & System Safety*, 206:107286, 2021.
- [9] Kai Cheng, Zhenzhou Lu, Chunyan Ling, and Suting Zhou. Surrogate-assisted global sensitivity analysis: an overview. *Structural and Multidisciplinary Optimization*, 61(3):1187–1213, 2020.
- [10] Hyoung-Seog Chung and Juan J. Alonso. Using gradients to construct cokriging approximation models for high-dimensional design optimization problems. In *40th AIAA Aerospace Sciences Meeting & Exhibit*, page 317, 2002.
- [11] Noel Cressie. The origins of kriging. *Mathematical geology*, 22(3):239–252, 1990.
- [12] Zhong-Hua Han, Stefan Götz, and Ralf Zimmermann. Improving variable-fidelity surrogate modeling via gradient-enhanced kriging and a generalized hybrid bridge function. *Aerospace Science and technology*, 25(1):177–189, 2013.
- [13] Zhong-Hua Han, Yu Zhang, Chen-Xing Song, and Ke-Shi Zhang. Weighted gradient-enhanced kriging for high-dimensional surrogate modeling and design optimization. *Aiaa Journal*, 55(12):4330–4346, 2017.
- [14] Robert Hecht-Nielsen. Theory of the backpropagation neural network. In *Neural networks for perception*, pages 65–93. Elsevier, 1992.
- [15] Sergei Kucherenko Ilya M. Sobol’. Derivative based global sensitivity measures. *Procedia-Social and Behavioral Sciences*, 2(6):7745–7746, 2010.

- [16] Donald R Jones, Matthias Schonlau, and William J Welch. Efficient global optimization of expensive black-box functions. *Journal of Global optimization*, 13(4):455–492, 1998.
- [17] James R. Koehler and Art B. Owen. 9 computer experiments. In Sumit Ghosh and Calyampudy Radhakrishna Rao, editors, *Design and analysis of experiments*, volume 13 of *Handbook of statistics*, pages 261–308. North-Holland, 1996.
- [18] Janusz S Kowalik and Michael Robert Osborne. *Methods for unconstrained optimization problems*, volume 13. Elsevier Publishing Company, 1968.
- [19] Danie G. Krige. A statistical approach to some basic mine valuation problems on the witwatersrand. *Journal of the Southern African Institute of Mining and Metallurgy*, 52(6):119–139, 1951.
- [20] Sergei Kucherenko, Balazs Feil, Nilay Shah, and Wolfgang Mauntz. The identification of model effective dimensions using global sensitivity analysis. *Reliability Engineering & System Safety*, 96(4):440–449, 2011.
- [21] Sergei Kucherenko and Shugfang Song. Derivative-based global sensitivity measures and their link with sobol’sensitivity indices. In *Monte Carlo and Quasi-Monte Carlo Methods*, pages 455–469. Springer, 2016.
- [22] Loic Le Gratiet. *Multi-fidelity Gaussian process regression for computer experiments*. PhD thesis, Université Paris-Diderot-Paris VII, 2013.
- [23] Weiyu Liu. *Development of gradient-enhanced kriging approximations for multidisciplinary design optimization*. University of Notre Dame, 2003.
- [24] Weiyu Liu and Stephen Batill. Gradient-enhanced response surface approximations using kriging models. In *9th AIAA/ISSMO symposium on multidisciplinary analysis and optimization*, page 5456, 2002.
- [25] Max D Morris, Toby J Mitchell, and Donald Ylvisaker. Bayesian design and analysis of computer experiments: use of derivatives in surface prediction. *Technometrics*, 35(3):243–255, 1993.

- [26] Richard D Neidinger. Introduction to automatic differentiation and matlab object-oriented programming. *SIAM review*, 52(3):545–563, 2010.
- [27] Nestor V Queipo, Raphael T Haftka, Wei Shyy, Tushar Goel, Rajkumar Vaidyanathan, and P Kevin Tucker. Surrogate-based analysis and optimization. *Progress in aerospace sciences*, 41(1):1–28, 2005.
- [28] Carl Edward Rasmussen. Gaussian processes in machine learning. In *Summer school on machine learning*, pages 63–71. Springer, 2003.
- [29] Benjamin Rosenbaum. *Efficient Global Surrogate Models for Responses of Expensive Simulations*. PhD thesis, Universität Trier, 07 2013.
- [30] Jerome Sacks, William J Welch, Toby J Mitchell, and Henry P Wynn. Design and analysis of computer experiments. *Statistical science*, 4(4):409–423, 1989.
- [31] Andrea Saltelli, Marco Ratto, Terry Andres, Francesca Campolongo, Jessica Cariboni, Debora Gatelli, Michaela Saisana, and Stefano Tarantola. *Global sensitivity analysis: the primer*. John Wiley & Sons, 2008.
- [32] Alex J Smola and Bernhard Schölkopf. A tutorial on support vector regression. *Statistics and computing*, 14(3):199–222, 2004.
- [33] Vladimir Vapnik. *The nature of statistical learning theory*. Springer science & business media, 1999.
- [34] Pengfei Wei, Zhenzhou Lu, and Jingwen Song. Variable importance analysis: a comprehensive review. *Reliability Engineering & System Safety*, 142:399–432, 2015.
- [35] Christopher K Williams and Carl Edward Rasmussen. *Gaussian processes for machine learning*, volume 2. MIT press Cambridge, MA, 2006.
- [36] Dongbin Xiu and George Em Karniadakis. The wiener–askey polynomial chaos for stochastic differential equations. *SIAM journal on scientific computing*, 24(2):619–644, 2002.

- [37] Liang Zhao, Peng Wang, Baowei Song, Xinjing Wang, and Huachao Dong. An efficient kriging modeling method for high-dimensional design problems based on maximal information coefficient. *Structural and Multidisciplinary Optimization*, 61(1):39–57, 2020.
- [38] Ralf Zimmermann. On the maximum likelihood training of gradient-enhanced spatial gaussian processes. *SIAM Journal on Scientific Computing*, 35(6):A2554–A2574, 2013.
- [39] Ralf Zimmermann. On the condition number anomaly of Gaussian correlation matrices. *Linear Algebra and its Applications*, 466(1):512–526, 2015.